Int. J. Hydrogen Energy, Vol. 15, No. 8, pp. 537–550, 1990.
Printed in Great Britain.

0360-3199/90 $3.00 + 0.00
Pergamon Press plc.
International Association for Hydrogen Energy.

ON ELECTROCHEMICAL TRITIUM PRODUCTION

G. H. LIN, R. C. KAINTHLA, N. J. C. PACKHAM, O. VELEV and J. O'M. BOCKRIS
Surface Electrochemistry Laboratory, Texas A&M University, College Station, TX 77843, U.S.A.

(*Received for publication* 18 *April* 1990)

Abstract—This paper reports tritium formed in LiOD–D_2O solutions in which Pd cathodes are used to evolve D_2. Electrolysis was carried out for up to $4\frac{1}{2}$ months. Excess heat has been observed from 5 electrodes out of 28, tritium in 15 out of 53 but 9 out of 13 if the electrodes are limited to 1 mm diameter. Steady state tritium concentrations were 10^4–10^7 disintegrations min^{-1} ml^{-1}. A weak correlation may exist between heat observed and tritium produced. The rate of production of tritium was *ca* 10^{10} atoms cm^{-2} s^{-1}. The branching ratio of tritium to neutrons was $\sim 10^8$. A theoretical dendrite enhanced fusion model is suggested. Growing gas layer breakdown occurs at sufficiently high surface potential dendrite tips and correspondingly fusion reactions occur. The model gives quantitative consistence with experiment, especially the sporadic nature and the observed branching ratio.

INTRODUCTION

Since Fleischmann, Pons and Hawkins [1] and Jones [2] reported the cold fusion phenomena, which is difficult to explain by conventional nuclear physics, several attempts to interpret the excess heat as well as radiative particle emission have been made. Such explanations fall into two large categories: chemical reaction and nuclear fusion. The heat released by a chemical reaction corresponds to the range of a few electron volts (eV) per atom in contrast to the energy liberated in a nuclear reaction—on the order of millions of electron volts (MeV) per nucleus. In an earlier paper [3], we summarized the eight possible chemical contributions to the excess heat seen in Ref. 1, and arrived at the conclusion that any chemical explanation would be improbable. No one chemical explanation will suffice to explain the magnitude of the excess heat observed, and the large amount of tritium produced in the solution and gas phases [4] cannot be explained by any kind of chemical reaction. The second category of explanation is a nuclear one. Different models to explain the cold fusion experiments have been suggested since they cannot be simply interpreted by today's nuclear physics.

There are two main characteristics of the cold fusion experiments. One is the large tritium to neutron ratio, on the order of 10^8, and the other is the sporadicity and irreproducibility of the phenomena. A suitable cold fusion theory or model must explain both of these features.

Proposed theories

Mayer [5] suggested that in prolonged electrolysis at high current density, internal cracks may appear and opposite charges may exist on the two sides of the crack. As the crack grows, the associated voltage drop would increase. A D^+ present in the void would thus be accelerated to high energy and then collide with another deuteron adsorbed on the void surface. This would lead to substantial tunneling. Correspondingly, Gajda [6] suggested that the high density pocket plasmas within the metal would lead to high temperatures and "hot" fusion.

Muon catalysed D–D nuclear fusion, triggered by cosmic rays, is another possible origin of cold fusion phenomena. If a muon is trapped by a deuteron, the internuclear distance of the two deuterium nuclei would be reduced by a factor of about 200, relative to the spacing of normal deuterium nuclei. The muomolecular ion then has a very large cross section for nuclear fusion, a secondary muon being produced. Thus, one muon may catalyse a large number of fusion events, e.g. 200, before it is eventually absorbed by a metal atom. However, in the experiment of Pd metal loaded with deuterium, placed in a muon beam, negative results were obtained [7], which may indicate that the absorption of muons by the Pd lattice is too large to catalyse nuclear fusion.

Another approach involves change of effective mass of electron or deuteron. Worledge *et al.* [8] suggested that in the Pd electrode, the effective mass of the absorbed deuteron could become 0.01 times the rest mass. The energy needed for a given probability of D–D fusion by tunneling through the Gamow barrier (Fig. 1) will be decreased by the same factor. Conversely, Jones [9] proposed a catalysed 'piezonuclear' fusion. The effective mass of the electron in the Pd electrode increases and this enhances the quantum penetration factor.

These models may not explain the two main characteristics of the "cold fusion" phenomena.

Isotopic enrichment

A large amount of tritium has been observed both in the solution and gas phases. Isotopic enrichment is not sufficient to explain the experimental results.

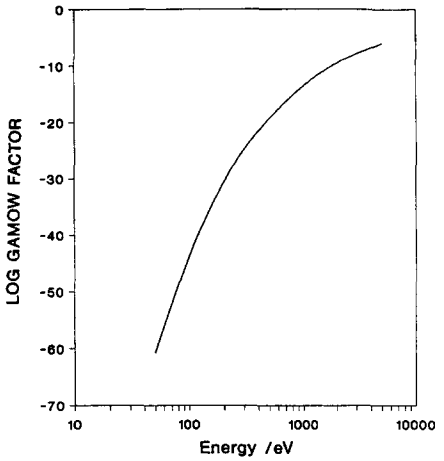

Fig. 1. The effect of energy on the Gamow penetration factor.

When deuterium oxide is electrolysed, the tritium concentration will increase because of the isotope separation effect [10]. There are two basic experimental set-ups. One involves a closed system, where deuterium and oxygen are recombined inside the cell. In this case, as no tritium is lost due to electrolysis and no fresh solution (containing trace amounts of tritium) is added, the tritium concentration remains constant in the absence of any nuclear reaction. Another set-up is an open cell, where deuterium and oxygen are allowed to escape freely into the atmosphere. Fresh D_2O containing about 200 disintegrations min^{-1} ml^{-1} of T is added at intervals of 12 to 24 h. Change in the tritium concentration will occur due to the addition of fresh D_2O containing T and due to removal by electrolysis. Let R be the rate of addition of fresh D_2O into the cell. This addition, in order to keep the volume V constant, must be equal to the rate of electrolysis of D_2O. Thus,

$$V\,dn_T(t)/dt = R\,n_T(0)/n - R_T \qquad (1)$$

where R_T is the rate of removal of tritium by electrolysis.

The isotopic separation factor of tritium to deuterium, is defined as

$$S = [R_D/R_T)/(n_D/n_T(t)] \qquad (2)$$

where R_D is the rate of production of deuterium atoms and n_D is the concentration of deuterium in the solution. According to Corrigan [11], $S = 1.7$–2.2 and will be taken as 2. Under the experimental conditions, $R_D \sim R$ and $n_D \sim n$, substitution of (2) into (1), and integration gives

$$n_T(t)/n_T(0) = S - (S-1)\exp(-t/\tau) \qquad (3)$$

with the tritium build-up time constant τ equal to

$$\tau = SnV/R. \qquad (4)$$

For a charging cell with a volume of 15 ml, and a total current of 0.15A, $\tau = 22$ days. In a calorimetric cell with a volume of 100 ml, and total current of 0.5A, $\tau = 44.4$ days.

The maximum tritium concentration in the solution due to isotopic separation at infinitely long times is S multiplied by the tritium concentration in the original solution, which is very small compared to the experimental results.

EXPERIMENTAL

(a) *Sources of electrode materials*

The 1 mm and 3 mm Pd cathodes used in the present study were cut from 99.9% pure rods made by Hoover and Strong (Richmond, VA) and purchased from the Texas Coin Exchange (College Station), while the 6 mm diameter electrodes were cut from the 99.9% pure rod purchased from Sure Pure Chemicals (NY). The 4 mm cathodes were cut from high purity "fusion" Pd on loan from Johnson Matthey. The lengths of the electrodes were about 4, 3, 2.5 and 2.5 cm, respectively.

Pt electrodes were of 99.9% purity, from Alfa Products (Danvers, MA), titanium (99.99%), from Johnson Matthey (Seabrook, NH) and Ni gauze (99.9%), from the Belleville Metals Company (Belleville, NJ).

Pure D_2O (99.9%) was obtained from Aldrich Chemical Co (Milwaukee, WI).

(b) *Pre-treatment*

After cutting to appropriate sizes, the electrodes were treated as described:

(i) No pre-treatment.

(ii) Acid etch. The electrodes were etched in 5 M HCl for 15 min, followed by rinsing in water and heavy water.

(iii) Annealing. The electrodes were annealed at 10^{-6} torr, at different temperatures between 800–1300°C for different times in an Edwards E306A vacuum system using a tungsten spiral heater. After cooling to room temperature, the vacuum chamber was filled to atmospheric pressure with argon. The electrode was removed from the heater, rubbed with abrasive paper and immediately transferred into a tube filled with D_2O.

(iv) Electrochemical. A Ni wire was spot welded to the electrode, which was then placed in a cell containing 0.1 M LiOD and Pt counter electrode. The electrode was cycled between +2 and −2 V for 2 h.

(v) Hammered. The electrodes were hammered to increase the dislocation concentration.

(vi) Electrodeposited Pd on Pd. In this case Pd was made a cathode in a cell containing 2% solution of $PdCl_2$ and Pd anode. Pd was deposited for about 10 min at a current density of 5 mA cm^{-2}.

(vii) Electroless Pd on Pd. In this case Pd electrode was left in $PdCl_2$ solution for about 24 h, during which time a black film of Pd was deposited on the electrode.

(c) *Charging*

After pre-treatment, a Ni wire was spot welded to the electrode. The electrode was introduced into a glass centrifuge tube containing appropriate electrolyte (Table 1) and the Ni mesh cylindrical electrode with Ni wire was spot welded to it. Charging was sometimes

Table 1. Sporadic observations of tritium and heat during D_2 evolution from D_2O on Pd

Cell	Electrode pretreatment	Solution	Tritium	Excess heat
A1 (1 mm)	No treatment	0.1 M LiOD	Yes	NM
A2 (1 mm)	No treatment	0.1 M LiOD + 0.1 mM NaCN	Yes	NM
A3 (1 mm)	Annealed, 800°C, 6 h	0.1 M LiOD	Yes	NM
A4 (1 mm)	Annealed, 800°C, 6 h	0.1 M LiOD + 0.1 mM NaCN	Yes	NM
A5 (1 mm)	Acid etch	0.1 M LiOD	Yes	NM
A6 (1 mm)	Acid etch	0.1 M LiOD + 0.1 mM NaCN	Yes	NM
A7 (1 mm)	Electrochemical	0.1 M LiOD	Yes	NM
A8 (1 mm)	Electrochemical	0.1 M LiOD + 0.1 mM NaCN	Yes	NM
A9 (1 mm)	No treatment, charged in U tube	0.1 M LiOD	No	Yes
M1 (1 mm)	No treatment	0.1 M LiOD	Yes	NM
M2 (1 mm)	Acid etch	0.1 M LiOD	No	NM
B1 (3 mm)	No treatment	0.1 M LiOD	No	No
B2 (3 mm)	No treatment	0.1 M LiOD + 0.1 mM NaCN	No	No
B3 (3 mm)	Annealed, 800°C, 6 h	0.1 M LiOD	Yes	No
B4 (3 mm)	Annealed, 800°C, 6 h	0.1 M LiOD + 0.1 mM NaCN	No	No
B5 (3 mm)	Acid etch	0.1 M LiOD	No	No
B6 (3 mm)	Acid etch	0.1 M LiOD + 0.001 M NaCN	No	No
B7 (3 mm)	Electrochemical	0.1 M LiOD	No	No
B8 (3 mm)	Electrochemical	0.1 M LiOD + 0.001 M NaCN	No	Yes
B9 (3 mm)	No treatment, charged in U tube	0.1 M LiOD	No	Yes
C8 (6 mm)	Electrochemical	0.1 M LiOD + 0.001 M NaCN	No	No
Cell 1 (6 mm)	No treatment	0.1 M LiOD	No	No
Cell 4 (3 mm)	Annealed, 1200°C, 12 h	0.1 M LiOD	Yes	Yes
JM1 (4 mm)	No treatment	0.1 M LiOD	No	No
JM2 (4 mm)	Annealed, 800°C, 24 h	0.1 M LiOD	No	No
Cell 4A (3 mm)	No treatment	0.1 M LiOD	No	No
H1 (3 mm)	Hammered; Electrochemical	0.1 M LiOD	No	No
AH1 (3 mm)	Annealed, 800°C, 8 h Hammered, Electrochemical	0.1 M LiOD	No	No
Cell 1A (6 mm)	Annealed, 800°C, 8 h	0.1 M LiOD	No	No
Cell 1B (3 mm)	Electrodeposited Pd on Pd	0.1 M LiOD	No	No
B5A (3 mm)	Annealed, 800°C, 24 h	0.1 M LiOD	No	No
The following samples are still being monitored				
Cell 4 (3 mm)	Earlier cell 4, new cell & solution	0.1 M LiOD	No	No
Cell 5 (6 mm)	No treatment	0.1 M LiOD	No	No
Cell 6 (3 mm)	No treatment	0.1 M LiOD	No	No
Cell 9 (4 mm)	JM1, annealed 1000°C, 8 h	0.1 M LiOD	No	No
Cell 10 (3 mm)	No treatment, Ni soldered to Pd	0.1 M LiOD	No	No
Cell 11 (6 mm)	Annealed, 1000°C, 8 hr	0.1 M LiOD	No	No
Cell 12 (3 mm)	Earlier AH1	0.1 M LiOD	No	No
A2 (1 mm)	Earlier A2, new cell & solution	0.1 M LiOD	No	NM
M2 (1 mm)	Earlier M2, new cell & solution	0.1 M LiOD	No	NM
B2A (3 mm)	Electroless Pd on Pd	0.1 M LiOD	No	NM
B3A (3 mm)	Electrodeposited Pd on Pd	0.1 M LiOD	No	NM
B4A (3 mm)	No treatment, Hammered	0.1 M LiOD	No	NM
B6A (4 mm)	Earlier JM2 new cell & solution	0.1 M LiOD	No	NM
B8A (3 mm)	Annealed, 1000°C, 12 h	0.1 M LiOD	No	NM
C2 (6 mm)	No treatment	0.1 M LiOD + 0.1 mM NaCN	No	NM
C4 (6 mm)	Annealed, 800°C, 6 h	0.1 M LiOD + 0.1 mM NaCN	No	NM

NM = No attempt made to measure.

carried out in polystyrene tubes with Pt mesh anodes. The Ni wires, from the Pd cathode and the anode, passed through a rubber septum. A stainless steel needle was introduced through the septum to allow D_2 and O_2 to escape. All the cells with 3 mm and 6 mm electrodes were connected electrically in series to a Hewlett Packard 6274B power supply while all the cells with 1 mm Pd cathodes were connected to a Hewlett Packard 6274B power supply in series. The charging current was ~ 64 mA cm^{-2} while the cell voltage was ~ 3.0–4.0 V. The cells were refilled with D_2O daily. In cells with Pt anodes, a recombination catalyst was introduced at the top, and the stainless steel needle removed. As there was no escape of gases in this case, there was no need to refill the cell with D_2O. The electrodes were left electrolysing D_2O for a few weeks to a few months. Sometimes, the Ni anode was repaired or replaced along with the solution and the glass tube.

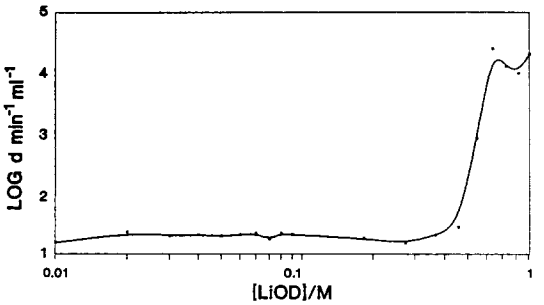

Fig. 2. The effect of electrolyte concentration on chemiluminescence of the scintillation cocktail [4].

(d) *Heat measurements*

After charging, for times varying from 1 to 25 weeks, the electrodes were transferred to a calorimeter for the measurement of heat.

The calorimeter used in the study was of the heat transfer type, and has been described elsewhere [12].

(e) *Tritium measurements*

Tritium analysis was performed on the alkaline electrolyte by *in situ* Liquid Scintillation Counting (LSC). Three counters were used. The first was a Wallac LKB model 1219 LSC; the second, a Wallac LKB model 1410, and the third an instrument constructed in the Cyclotron Institute. A water soluble scintillation cocktail (Biosafe II, Research Products International Corporation, 15 ml) was added to 1 ml of sample, and allowed to stand under cover for 30 min before counting. This was found to eliminate the chemiluminescence contributions (for concentrations of LiOD < 0.2 M). The samples were analysed in a double-blind fashion (with respect to the operator of the counter). Multiple blank samples of H_2O, D_2O, and 0.1 M LiOD were included for analysis. A test for chemiluminescence was made using samples ranging from 1 to 0.01 M LiOD, including samples that had been neutralized by potassium hydrogen phthalate. Results are shown in Fig. 2. Samples run 24 h later showed no significant change in activity levels. The efficiency of the model 1219 detector for tritium in the samples was 33%, for the model 1410 around 40%, and for the counter constructed in the Cyclotron Institute, around 30%. One minute and 10 min analyses (some samples were run overnight) were performed. A detailed analysis of the energy spectra from the Cyclotron Institute counters yielded the correct β energy end point for tritium (18 keV) (cf. Fig 3B and B).

The results are shown in Table 2, and are given as counts per minute (cpm) per ml of sample, and as disintegrations per minute (dpm) per ml of samples. At low count rates, the random errors in counting were up to 7%, whilst at high count rates, this figure dropped to 2%. The conversion factor for calculating background-corrected rates is given by:

$$\text{dpm ml}^{-1} = (\text{cpm ml}^{-1}_{\text{sample}} - \text{cpm}_{\text{cocktail}}) \times (V/E) \quad (5)$$

where E is the efficiency of the detector and V is the volume factor to give results per ml of sample.

After the analyses at Texas A&M,* the tritium content of the liquids resulting from the electrolyses, including a tritium (HTO) standard and blanks of LiOD and D_2O, was examined by Los Alamos National Laboratory (National Tritium Center), Argonne National Laboratory, Battelle Pacific Northwest Laboratory and the General Motors Research Laboratory. These results are shown in Table 3.

(f) *Examination of blanks and matters related to contamination*

The possibility that large amounts of tritium were present in either the D_2O or the Li used to make the LiOD, is ruled out by the results of Table 4(a) and (b). Each batch of D_2O that was used for refilling the cells was analysed for tritium content, both on the 1219 instrument (Table 4a), and the 1410 (Table 4b, shown as a mean of 10 results). Many experiments were run in which no significant increase of tritium was observed, including identical cells to the ones which did produce tritium, except for the electrolyte, which was 0.1 M

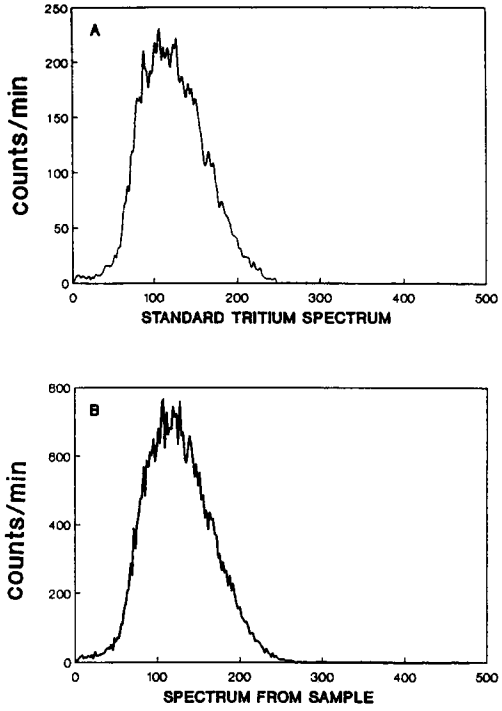

Fig. 3. (A) The spectrum of a tritiated water sample. (B) A representative spectrum obtained from an electrolyte sample.

*The initial analyses at Texas A&M were carried out by Dr Kevin Wolf, Dr Milton McClain, Mr Peter Lee, and the Health Physics Group, to whom we give our appreciation.

Table 2. Cell identification, electrode treatment, solution type and tritium activity of electrolyte samples

Cell	Electrode pretreatment	Solution	Corrected ^3H activity (dpm ml^{-1})
A1	No treatment	0.1 M LiOD	3.8×10^4
A2	No treatment	0.1 M LiOD + 0.1 mM NaCN	
	After 16 days at 50 mA cm^{-2} then for 8 hours at 500 mA cm^{-2} (5/1/89)		168
	50 mA cm^{-2} for 4 days (5/5/89)		134
	50 mA cm^{-2} for 3 h, 100 mA cm^{-2} for 2 h, 200 mA cm^{-2} for 20 min (5/6/89)		1.1×10^4
	50 mA cm^{-2} (5/7/89)		1.4×10^4
	(5/7/89—5/13/89)		1.1×10^4
	(5/13/89—6/6/89)		7.5×10^3
A3	Anneal	0.1 M LiOD	4.9×10^6
A4	Anneal	0.1 M LiOD + 0.1 mM NaCN	1.2×10^5
A5	Acid etch	0.1 M LiOD	3.7×10^6
A6	Acid etch	0.1 M LiOD + 0.1 mM NaCN	3.3×10^4
A7	Electrochemical	0.1 M LiOD	
	Before high current density		102
	After 2 h at 500 mA cm^{-2}		5223
	After 6 h at 500 mA cm^{-2}		5.0×10^5
	After 12 h at 500 mA cm^{-2}		7.6×10^5
A8	Electrochemical	0.1 M LiOD + 0.1 mM NaCN	
	After 16 days charging and 8 h high current density (5/1/89)		192
	Electrolyte levels after 6 weeks at 50 mA cm^{-2}		5.0×10^5
	Recombined gas levels after 2 weeks of external recombination at 50 mA cm^{-2}		5.0×10^7
B3 (3 mm)	Anneal	0.1 M LiOD	6.3×10^4
B5 (3 mm)	Acid etch	0.1 M LiOD	48
Cell 1 (6 mm)	No treatment	0.1 M LiOD	117
Cell 4		See Fig. 6	
M1	No treatment	0.1 M LiOD	3000

Table 3. Confirmatory results from outside sources on various samples corrected ^3H activity in dpm ml^{-1}

Sample	Cell 1	Cell 2	HTO Standard	0.1 M LiOD	D_2O
Institution					
Texas A&M	2.13×10^6	1157	7.23×10^5	93	47
Battelle	1.96×10^6	1170	8.08×10^5	127	140
Argonne	1.96×10^6	1020	7.59×10^5	90	114
Los Alamos	1.97×10^6	800–1300	6.50×10^5	113	161
General Motors	1.80×10^6	1000	--------Not analysed--------		

LiOH in H_2O (Tables 4b and 5).* Possible contamination from the nickel anode was examined by dissolving an unused piece of nickel from the same sheet used for all counter electrodes in concentrated nitric acid, followed by neutralization and then counting, with negative results.

Samples of virgin palladium and nickel of the same batch used for all 1 mm Pd cells were sent for analysis to Los Alamos National Laboratory, with no tritium being detected. In addition, palladium was used throughout as a cathode, the electrochemical nature of which would tend to drive H (D, T) into the cathode, rather than evolve tritium from within the electrode.

Secret interference is considered improbable because positive results from the Cyclotron Institute are in a part kept locked. No supplies of tritium are in the Cyclotron Institute. Inadvertent contamination is unlikely. No previous tritium work has been performed in the laboratories involved.

In addition, if it is supposed that the Pd had, earlier in its history, suffered prolonged exposure as a cathode in D_2O, T would have diffused into the electrode. Simple calculation shows [13] that it would take $< 10^2$ h to diffuse out again for a Pd rod kept in air.

Wires have, of course, been made from Pd which has passed through a molten state during manufacture.

*However, no light water solutions were examined for more than 6 weeks.

Table 4.(a) Blank experiments during tritium analysis performed on the 1219 counter

Sample	cpm ml^{-1}	Background corrected activity (dpm ml^{-1})
D_2O Analysis # 1	65	48
D_2O Analysis # 2	70	63
D_2O Analysis # 3	67	54
D_2O Analysis # 4	60	33
D_2O Analysis # 5	50	3
D_2O Analysis # 6	71	66
D_2O Analysis # 7	75	78
D_2O Analysis # 8	62	39
0.1 M LiOD analysis # 1	75	78
0.1 M LiOD analysis # 2	70	63
0.1 M LiOD analysis # 3	74	75
0.1 M LiOD analysis # 4	65	48
0.1 M LiOD analysis # 5	60	33
0.1 M LiOD analysis # 6	66	51
0.1 M LiOD analysis # 7	76	81
0.1 M LiOD analysis # 8	70	63
Neutralized 0.1 M LiOD	73	72
Neutralized 0.1 M LiOD + 0.1 mM NaCN	76	81
Dissolved nickel in acid analysis # 1	78	87
Dissolved nickel in acid analysis # 2	80	93
Dissolved nickel in acid analysis # 3	76	81
Scintillation cocktail	49	—

Table 4.(b) Mean of 10 blank experiments during tritium analysis performed on the 1410 counter

Sample	cpm ml^{-1}	Background corrected activity (dpm ml^{-1})
Biosafe II Cocktail	170 ± 13	—
H_2O Analysis	161 ± 16	0
D_2O Analysis	210 ± 16	100
0.1 M LiOD analysis	220 ± 20	125
0.1 M LiOH analysis	157 ± 12	0
Dissolved nickel in nitric acid	140 ± 20	0
Tygon tubing in NaOH	105 ± 20	0
Rubber stoppers in NaOH	150 ± 20	0
Recombination catalyst in NaOH	140 ± 15	0
Dissolved shavings from cutters	160 ± 11	0
Dissolved shavings from vacuum chamber	164 ± 17	0
Dissolved shavings from spotwelder	155 ± 10	0

Finally, some of the electrodes which gave tritium had been heavily annealed just prior to immersion in the D_2O–LiOD. Thus, contamination would seem unlikely.

EXPERIMENTAL RESULTS

(1) *Reproducibility and repeatability*

The special difficulty of the present work is poor repeatability. Table 1 summarizes some of the results of heat and tritium measurements on all the electrodes studied so far in this laboratory. Excess heat has been observed in only 5 out of the 28 electrodes, tritium in 15 out of 53. The observation of tritium with 1 mm diameter wires has been more successful with 9 out of 13 1 mm electrodes yielding tritium. None of the seven 6 mm electrodes have shown any excess heat or tritium for observation periods of up to 6 months. Both heat and tritium has been observed together only for one electrode. However, in some half of the present work, heat and tritium were not regularly recorded together. Further, heat and tritium come in bursts. T may have been produced during some heat bursts (as DT) and sparged out before measurement was made. The duration of the experimental work covered in this paper is about 25 weeks.

(2) *Rise times during switch-on*

In one of the cells (cell A7, cf. Table 2) the build up of tritium as a function of time was followed at high current density. The results shown in Fig. 4 indicate either the time for reaching equilibrium of DT in solution to DT in the gas over the solution; or represent

Table 5. Details of cells that produced no tritium with 1410 LSC (corrected activity)

Experiment	dpm ml^{-1}
3 mm × 3 cm Ti Cathode in 0.1 M LiOD with internal gas recombination	275
3 mm × 3 cm Pd Cathode in 0.1 M LiOD with internal gas recombination	235
3 mm × 3 cm Ti Cathode in 0.1 M LiOD with internal gas recombination	285
0.5 mm × 1 cm Pd Cathode in 0.1 M LiOD with internal gas recombination	55
4 mm × 2 mm Pd disc Cathode in 0.1 M LiOD with internal gas recombination	365
0.5 mm × 1 cm Pd Cathode in 0.1 M LiOD with external gas recombination (recombined gases measured)	315
1 mm × 4 cm Pd Cathode in 0.1 M LiOD with external gas recombination (recombined gases measured 7/18/89)	75
1 mm × 4 cm Pd Cathode in 0.1 M LiOD with external gas recombination (recombined gases measured 7/21/89)	33
1 mm × 4 cm Pd Cathode in 0.1 M LiOH (H_2O) No gas recombination	0
1 mm × 4 cm Pd Cathode in 0.1 M LiOH (H_2O) No gas recombination	18

the time in which a burst occurred, the product being largely DTO.

(3) *Fall time during switch-off*

Another cell (cell A2 in Table 2) was tested for tritium over an extended period of time. It was run at a low current density for 16 days, followed by a 10 h period at high current density, after which, tritium was not produced. The cell was then transferred to the Cyclotron Institute where it remained at low current density for another week, with no tritium production. On 6 May, the current was increased to 110 mA cm^{-2} for 2 h, increased again to 300 mA cm^{-2} for 20 min, decreased to 90 mA cm^{-2} for seven days then returned to 50 mA cm^{-2} until 22 June. The tritium content of the solution was monitored during this time and the results are shown in Fig. 5, which indicates the production period was about 2 days, and the decay period about 3 days.

(4) *The steady state tritium values*

The steady state concentrations in T producing cells varied between 10^4 and 5×10^6 dpm ml^{-1}. These are shown in Table 2.

(5) *Pre-treatment and degree of tritium production*

Details on the pretreatment of the electrodes that produced tritium are given in Table 1.

The cell 4 electrode, the only electrode which has shown excess heat twice and two tritium bursts, was

*It is unlikely that the error involved in this assumption is >2. At the present juncture, our ability to calculate modelistically is no better than ± 10×.

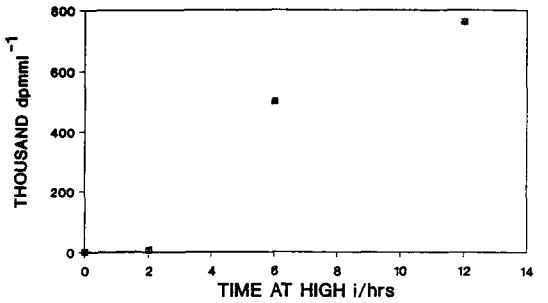

Fig. 4. The production of tritium in the electrolyte of cell A7 as a function of time [4].

vacuum annealed at 10^{-6} torr at 1200–1300°C for 12 h. The excess heat was observed for the first time after about 3.5 months, while the combined tritium and excess heat were observed after about 4.5 months of electrolysis.

(6) *Correlation of tritium production to heat*

Some relation between heat and tritium production is indicated qualitatively by the shape of the relation shown in Fig. 6.

If the tritium is in the solution in the form of DT, it should be subject to physicochemical laws of vapor pressure equilibrium, i.e. it should be present in the gas phase according to Henry's Law.

Henry's law states that the mole fraction (x) of solute is given by

$$x = p/K \tag{6}$$

where p is the partial pressure and K is Henry's law constant. For H_2 in H_2O the value of K is 5.3×10^7 mmHg. As the value for T_2 or DT in D_2O is not known,* we will take the applicable value as 5.3×10^7 mmHg.

The disintegrations $min^{-1}\,ml^{-1}$ are equivalent to *ca* 10^{12} atoms ml^{-1}, using equation (6) and assuming the heat comes from $D + D \rightarrow T + H + 4.02$ MeV, the corresponding heat is about 3 W cm^{-2}, the same order as the heat being produced.

On the other hand, in the experimental measurements of the cell in which both heat and tritium production were observed, excess heat was observed for about ten

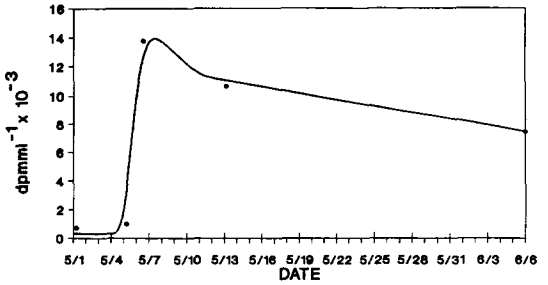

Fig. 5. The production of tritium in the electrolyte of cell A2 as a function of time (ordinate gives date) [4].

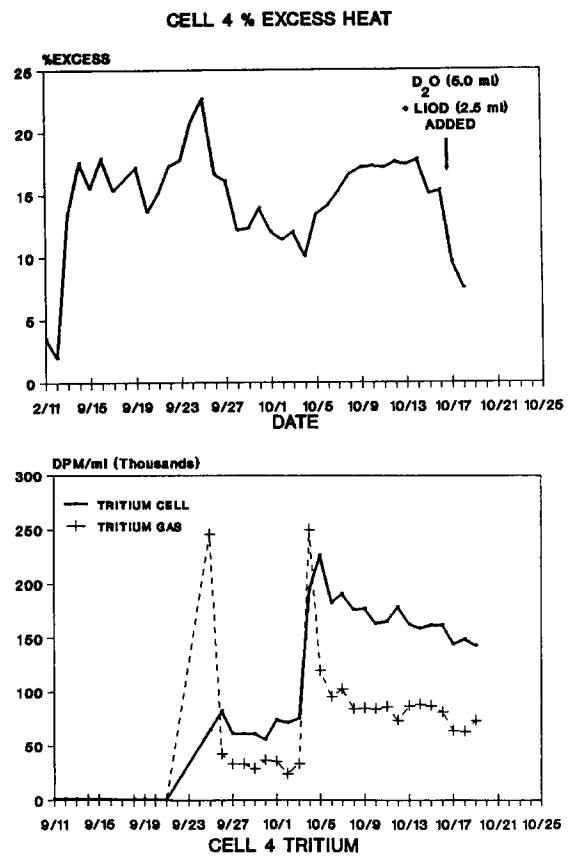

Fig. 6. The heat measurements and tritium activity levels from cell 4 showing a possible correlation between the two.

days before any increase in tritium concentration (Fig. 6). Tritium was then produced for around 7 days. For another eight days, during which time the electrode combined to show excess heat, no further increase in the tritium concentration was observed. Then, the tritium concentration increased by a factor of about 4. The amount of tritium produced can be determined from the total number of disintegrations measured. Thus, the amount of tritium produced during the above two occasions was 8×10^{13} and 1.8×10^{14} atoms, which correspond to rates of tritium production of 2.28×10^{8} and 1.16×10^{9} atoms s^{-1}, respectively (the time taken for the calculation is 4 days (or 96 h) for the first event and 1 day (or 24 h) for the second event. Knowing that the reaction producing each tritium atom is accompanied by 4.02 MeV energy, the heat produced in these events corresponds to 1.46×10^{-4} and 8.9×10^{-4} W, respectively. (In the first instance, the time could be much less.) However, the excess heat produced during the times the bursts were observed was in the range of 0.3 to 0.6 W.

*In Fe, such voids have been measured at overpotentials near zero to have dimensions of about $1000 \times 100 \times 100$ Å [17].

Thus, the amount of tritium produced can account, on the assumption that it gives heat on the basis of $D + D \rightarrow T + H + 4.02$ MeV, for only $\sim 0.1\%$ of the excess heat. The total amount of excess heat produced during the operation of the cell hitherto is several MJ.

The direct approach to the total heat is inconsistent with the indirect one, the explanation may be that the T formed in a nuclear process on the electrode were sufficiently energetic to form DTO in the solution. If 99.9% of the T formed DTO, the results measured by the recombination catalyst (external DTO formed by combustion) will be explicable. The heat would then be only 0.1% of the observed heat (for the total T production would be essentially what is observed in the solution).

OTHER PHENOMENOLOGICAL ASPECTS

(1) *Production rate of tritium*

The rate of tritium production is 2×10^{8}–2×10^{9} atoms s^{-1} for the first and second bursts in the experiment, respectively. The maximum rate we observed is about 10^{10} atoms s^{-1}.

(2) *Branching ratio*

The tritium production rate is about 10^{9} atoms s^{-1} cm^{-2} from our experiments. Neutron bursts have been observed by Wolf *et al.* [14], at the level of 1 to 2 s^{-1} cm^{-2}. Thus, the branching ratio is on the order of 10^{9}. However, other results [15, 16], shows that the neutron production rate may be about 10^{2} s^{-1} cm^{-2}. Thus, on this basis, the branching ratio would be $\sim 10^{7}$.

(3) *Comparison of standard tritium sample to those of* T *in solution*

The spectrum from a standard tritium sample is shown in Fig. 3(A). Below it (Fig. 3B), is shown a spectrum for one of the experiments carried out by K. Wolf [14]. The spectra show β end point energies of 18.6 keV, the value for tritrium.

ELECTROCHEMICALLY PRODUCED TRITIUM FOUND BY OTHER WORKERS

The results of other workers who have found tritium, as well as the activities found, are shown in Table 6.

FUSION MODELS IN ELECTROCHEMICAL CONFINEMENT

(1) *High fugacity*

The classical electrochemical calculation of the fugacity of molecular hydrogen in voids* in the metal assumes that this hydrogen must be at a fugacity which would be necessary to give the electrode a reversible potential

Table 6. Other workers' tritium results

Group	Activity (dpm ml^{-1})	Comments
Yeager and Adzic, Case Western Reserve	10^4	5× Background Several Times
Schoessow and Wethington, U. of Florida, Gainesville	10^5	2 cells only
Ramirez, Mexican Institute of Petroleum	10^3	1 cell of 3
Packham *et al.*, Texas A&M University	10^4–10^7	See Table 1. One with heat
Wolf *et al.*, Texas A&M University	10^6	1 cell
Iyengar, BARC	10^5	Many occasions
Storms and Talcott, Los Alamos National Lab	10^3	2 cells of 91 also 9 at 400
Guruswamy *et al.*, National Cold Fusion Institute	Variable	Several Occasions
Scott *et al.*, Oak Ridge	10^4	1 Cell
Adams *et al.*, University of Ottawa	Unknown	
Alqasmi, Arab Emirates Univ.	Unknown	
McBreen *et al.*, Brookhaven Nat. Lab.	Unknown	
Claytor *et al.*, Los Alamos National Lab	Unknown	
Scaramuzzi *et al.*, Frascatti, Italy	Unknown	
Sanchez *et al.*, Madrid, Spain	10^3	Qualitative correlation with γ

equal to its overpotential. The potential of a thermodynamically reversible hydrogen electrode is related to the fugacity of the hydrogen by the equation:

$$V_{\text{Rev. 2}} = V_{\text{Rev. 1}} - \frac{RT}{2F} \ln p_{D_2} \tag{7}$$

$$(f_{D_2})_{\text{voids}} = f_{D_2(\text{atm})}\, e^{-2\eta F/RT} \tag{8}$$

where $V_{\text{Rev. 1}}$ is the potential at a deuterium pressure of 1 atmosphere, $V_{\text{Rev. 2}}$ is the potential at pressure p, η is the overpotential in the negative direction due to the high fugacity (f) of D_2 formed in voids in the metal. Thus, from equation (8): Suppose, at 1 A cm^{-2}, η_{D_2}(Pd) is -0.6 V, then ($F_{D_2})_{\text{voids}} = 10^{20}$ atm.

However, the reasoning given [1] which uses such calculations to infer huge pressures leading to fusion involves two difficulties.

(i) The deuterium overpotential at $i = 1$ amp cm^{-2} is $\ll 0.6$ V and hence, following (8), $p_{D_2} \gg 10^{20}$ atm. However, [18] if:

$$(p_{D_2}) > \left(\frac{16}{3}\frac{Y\gamma}{l}\right)^{1/2} \tag{9}$$

the void will become unstable and spread. Here, Y is Young's modulus, γ is the surface tension of Pd and l is the length (or radius) of the void. Typical values here would be around: $Y = 10^{12}$ dynes cm^{-2}; $\gamma = 10^3$ dynes cm^{-1}; $l = 10^{-5}$ cm. With these values, the value p_{D_2} at which the voids will become unstable is about 10^4 atm. Thus, for the actual η values of < -0.6 observed on Pd at high current densities, p_{D_2} in internal voids would exceed the spreading pressure, the voids would grow and the pressure sink.

(ii) Apart from such numerical consideration it is not valid to use an equilibrium thermodynamic approach which underlies equations (7) and (8). The relation of hydrogen fugacities to overpotential corresponding to various mechanisms of H_2 evolution calculated to a kinetic basis, are given in Table 7. Thus, the fugacity associated with a given overpotential depends on the mechanism of deuterium evolution. For high current densities and alkaline solutions on Pd, this has not been determined. However, it is likely by analogy to knowledge of hydrogen evolution on Pt that, at low current densities (up to 10 mA cm^{-2}, say), $\theta_D \ll 1$ and the rate

Table 7. Summary of the internal pressure calculation as a function of the mechanism of the hydrogen evolution reaction

Mechanism	Fugacity f_{H_2} (atm)	Remarks
Fast discharge slow combination	$\exp\{-2\eta F/RT\}$	Nernst equation valid could be embrittling
Slow discharge fast combination	1	Non-embrittling
Slow discharge–fast electrochemical desorption	$\exp\{2\eta F/RT\}$	Non-embrittling
Fast discharge–slow electrochemical desorption	$\exp\{-2\eta F/RT\}$	Nernst equation valid could be embrittling
Coupled-discharge combination	$10^{1.5} \times \exp\{-\eta F/2RT\}$	$\theta \ll 1$ could be embrittling
Coupled-discharge electrochemical desorption	$\exp\{-2\eta^* F/RT\}$	only predictable exactly if η^* is known experimentally.†

†η^* represents the potential at which fast-discharge-electrochemical desorption changes to coupled-discharge-electrochemical desorption.

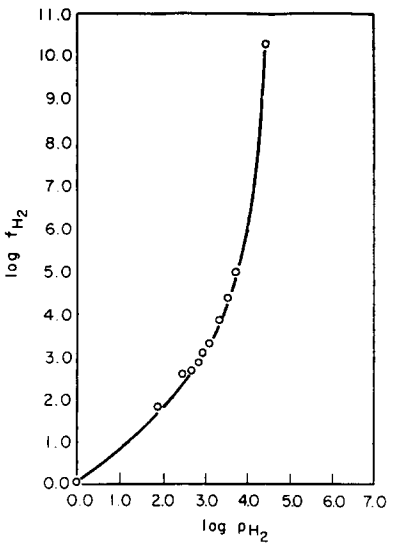

Fig. 7. The relationship between fugacity and pressure [17].

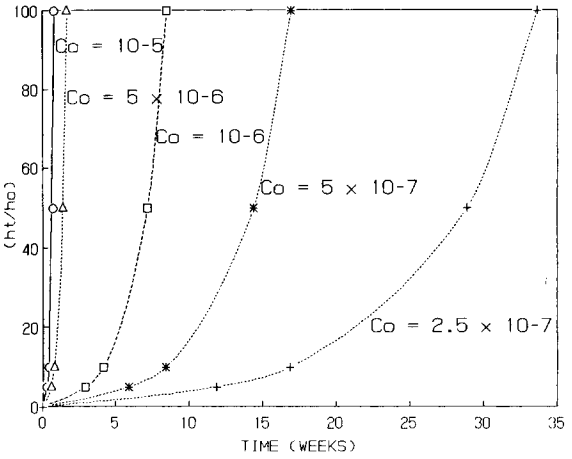

Fig. 8. The growth of promontories on the surface of electrodes as a function of time and impurity concentration.

determining step is surface chemical recombination of D to D_2 (whereupon, an equation similar to (8) would be applicable). Conversely, at sufficiently high c.d.'s, θ_D approaches unity. Then, chemical combination would no longer be the r.d.s. This would become the coupled discharge electrochemical desorption, $D_2O + D_{Ads} + e \rightarrow D_2 + OD$.

Then [19]:

$$f_{D_2} = (f)_0 e^{-\eta^x F/2RT} \quad (10)$$

where η^x is deuterium overpotential at which the rate determining step changes from the Tafel step to that of Heyrovsky. Again, by analogy to Pt, it is likely that this occurs at about -0.3 V.

As the overpotential continues to become more negative, with the coupled discharge electrochemical desorption step rate determining, no further increase of fugacity within the lattice would occur (become $\theta_D = 1$).

Hence, the highest possible fugacity would be [from equation (10)]:

$$(f_{D_2})_{max} = 10^6 \text{ atm}.$$

The corresponding pressure (Fig. 7) is:

$$p_{D_2} \sim 10^3 \text{ atm}$$

and the metal would remain largely unembrittled.

However, fusion by internal confinement requires around 10^{10} atm [20]. As it has been shown that Pd cannot (mechanically) stand pressures of $> 10^4$ atm without cracking, and the coupled discharge-electrochemical desorption mechanism is r.d.s. and will give f_{D_2} only up to *ca* 10^6 atm, fusion as a result of high internal fugacities of D_2 in Pd in unlikely.

(2) *The switch on time*

The time (10^2–10^3 h) needed to commence the production of tritium is much longer than the time needed to charge (e.g.) a 1 mm rod, and shows a variation and sporadic behavior difficult to justify on the internal pressure view.

Thus, using the formula:

$$\Delta^2 = 2Dt \quad (11)$$

where D is the diffusion coefficient (1.5×10^{-6} cm^2 s^{-1} for the α phase and 1.6×10^{-7} cm^2 s^{-1} for the β phase [21]), Δ is the radius of the rod (cm) and t is the time. Hence for a 1 mm diameter rod, $t = 2.4$ h. For a 3 mm rod, $t = 22$ h.

These times are *ca* 100 times lower than the actual times observed for the switch-on of the production of T. This discrepancy therefore speaks against high internal fugacity as a prerequisite to tritium production [1].

Promontories, some dendritic, grow gradually on electrodes during prolonged electrolysis. An equation governing the time of growth of such promontories under diffusion control [22] runs:

$$h_t/h_0 = e^{(tVDC_0)/\delta^2} \quad (12)$$

where h_t is the height of the promontory after time t, and h_0 that at the commencement of electrolysis, t is the time in seconds, V is the molar volume of the electrode material (8.8 cm^3 for Pd), D is the diffusion coefficient of the alleged depositing ionic impurity in cm^2 s^{-1}, C_0 is its concentration in moles cm^{-3}, and δ is the diffusion layer thickness in cm. For a moderately stirred solution, δ can be taken as 0.01 cm, and D as 10^{-5} cm^2 s^{-1}. Using these values, Fig. 8 shows the variation of (h_t/h_0) with time for various concentrations of the impurity. The reasonable parameters chosen make it possible for the take-off time of growth to vary in the range 10–100 weeks.

(3) *A new hypothesis*

In Fig. 8, the take-off time for the growth of promontories occurs at times between 2 and 100 days for assumed impurity concentrations in the range 10^{-7}–10^{-5} M. It is the time at which rapid increase of dendritic

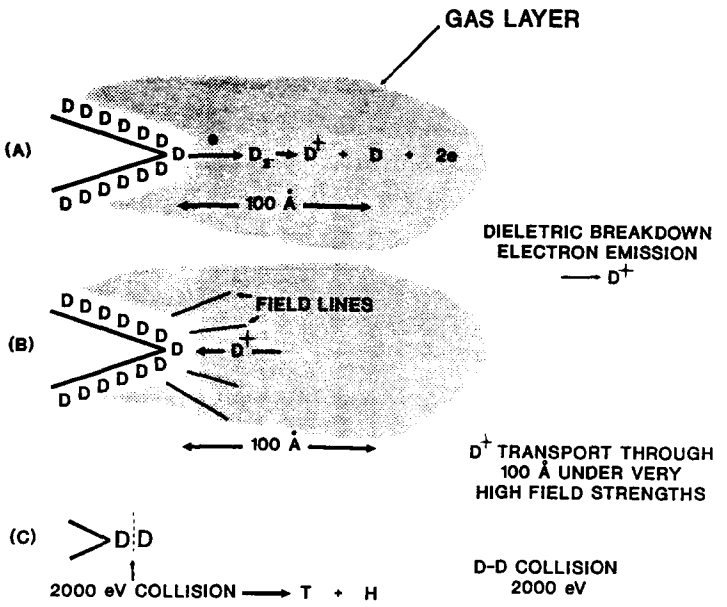

Fig. 9. Dielectric breakdown on a gas covered dendrite tip.

growth begins which fixes the time at which the production of tritium commences. The "impurity" is likely to be the anode material but a surprising number of metals on the cathode have been observed on the electrode after prolonged electrolysis [23]. These are the most likely places where high electric fields or high stress fields may develop which make fusion more probable.

Such a hypothesis is consistent with the sporadicity of the effects, and the variety of the nature of the cathode deposits. Large electrodes would tend not to produce tritium. Their surface area getters the solution of impurities before the transition time for rapid dendrite growth has been reached.

(4) *Values of the electric field*

The electric field in the double layer at an electrode is usually taken as having an order of magnitude of $10^8\,\mathrm{V\,cm^{-1}}$. However, recently Kolb and Franke [24] have concluded that it can be $\sim 10^9\,\mathrm{V\,cm^{-1}}$ in certain areas. The enhancement is due to surface states on the electrode which concentrate the field lines near these states.

The tips of dendrites are the points at which local dielectric breakdown is likely. It seems reasonable to accept values for the local double layer field of $> 10^9\,\mathrm{V\,cm^{-1}}$. There is no simple method of calculating the enhancement in field due to the dendrite tip. It will therefore be assumed (somewhat conservatively) that this serves to double the large values of the field deduced by Kolb and Franke [24].

(5) *Dielectric breakdown*

The breakdown of the water dielectric is likely to begin at sharp points (i.e. the dendrite tips) on the electrode surface, and thereafter a D_2 gas layer will be formed at the surface [25] (Fig. 9). When the gas layer grows, a transient large electric voltage drop may be developed on the dendrite tips. Electron emission will occur from dendrite tips into the gas, and in the gas layer the breakdown reaction:

$$D_2 + e \rightarrow D^+ + D + 2e \qquad (13)$$

seems feasible. Indeed, dark blue sparks have been seen in certain electrolysing cells.

The D^+ produced will be pulled by the field lines through the gas to the cathode surface on the nearest available surface, the dendrite tip. Such a surface will be likely to retain adsorbed D with which the D^+ would be expected to collide.

The D^+ path length may be of the order of the thickness of the gas layer, *ca* 100 Å. Hence, the transient voltage drop would be about 2000 eV.

(6) *Comparison of theory with experiment*

Suppose i is the current density in $\mathrm{A\,cm^{-2}}$, then $N_A i/F$ is the number of D–D collisions on the electrode surface* in atoms $\mathrm{cm^{-2}\,s^{-1}}$, where F is the charge on one gram ion, in coulombs.

Let it be supposed that a fraction, Γ of the surface is occupied with sharpened tip material. Then, let the probability of tunneling at such places be P_T, equivalent to:

$$P_T = \exp\{-\pi e_0^2 M^{1/2}/\hbar E^{1/2}\} \qquad (14)$$

*The collisions arise in the Volmer–Heyrovsky mechanism due to D_2O discharging a proton onto an adsorbed D to give D_2.

Therefore, the rate of T formation in atoms $sec^{-1}\,cm^{-2}$ is given by:

$$\Gamma(i/F)P_T. \tag{15}$$

In Table 8 and Fig. 1, this function is tabulated for $i = 1\ A\,cm^{-2}$ and $\Gamma = 10^{-3}$. It is seen that the calculated fusion rate is about 2×10^6 compared with the experimental rate of 10^8 to 10^{10} atoms $cm^{-2}\,s^{-1}$.

(7) *Further considerations*

Quantitative agreement with the model can be obtained by doubling the field to allow for its concentration at a sharp point. The assumption that Γ might be $\sim 10^{-3}$ is based on the appearance of the electron microscope pictures of Pd electrodes after prolonged electrolysis. It is possible that $\Gamma < 10^{-3}$, reducing the degree of agreement.

On the other hand, quantitative treatments of two factors neglected in this first approach would tend to increase the rate.

(i) The double layer involves electron overlap [26]. The electron cloud existing at the tip of the dendrite acts as a screen and reduces repulsion. Correspondingly, the adsorbed deuteron is shielded by the loss of cationic character.

(ii) Recently, Y. E. Kim [27] has shown that elcctron screening may reduce the needed collision energy from 4000 to *ca* 200 eV. Of course, if this assertion is correct, the present model is made more likely. It would be possible to dispense with the reliance on the specially high electric fields arising from the work of Kolb and Franke and use those normally seen by electrochemists, i.e. 10^7–$10^8\ V\,cm^{-1}$.

(iii) Worledge *et al.* [8] have suggested that the effective mass of the deuteron is less than the rest mass in a force-free field. On this basis, the needed E in the Gamow expression declines in proportion to the reduction of M_D. At $M_D = 0.01$, [8] $4 \times 10^7\ V\,cm^{-1}$ would give agreement with experiment and this is generally available in the electrical double layer at electrodes without the enhancement arising from low radius dendritic tips.

(8) *Decrease of Fleischmann–Pons effects with increase of electrode size*

Table 1 shows that smaller electrodes—those having diameters of 1 mm—are much more likely to give tritium than those which are larger, e.g. 4–6 mm diameter. Correspondingly, Srinivasan and Appleby [28] have found that excess Fleischmann–Pons heat is observed at small electrodes regularly but on larger ones decreasingly.

Table 8. The relationship between required energy and the fusion rate, f

E (eV)	G	$f(i = 1A\,cm^{-2})$	$f\Gamma\,(i = 1A\,cm^{-2})$
1000	2.63×10^{-14}	1.64×10^5	1.64×10^2
1500	8.18×10^{-12}	5.11×10^7	5.11×10^4
2000	2.50×10^{-10}	1.56×10^9	1.56×10^6
2500	2.59×10^{-9}	1.61×10^{10}	1.61×10^7
3000	1.44×10^{-8}	9.00×10^{10}	9.00×10^7
3500	5.52×10^{-8}	3.45×10^{11}	3.45×10^8
4000	1.62×10^{-7}	1.01×10^{12}	1.01×10^9

The switch-on time for the dendrite growth is

$$\tau_{Den} > \delta^2/DC_0V_{met}. \tag{16}$$

However [29], for gettering of the impurities from a solution:

$$C_t/C_0 = e^{-DAt/\delta V_{sol}}. \tag{17}$$

Therefore, the switch-on time for gettering is:

$$\tau_{get} > \delta V_{sol}/DA. \tag{18}$$

If the time at which the gettering action switches on is less than that at which the dendrites growth starts, the impurities will be removed from the solution and no dendritic growth will occur.

Therefore for successful tritium formation

$$\tau_{get} > \tau_{Den} \tag{19}$$

or

$$V_{sol}V_{met}C_0/\delta A > 1. \tag{20}$$

Hence, the larger A, the greater must be the concentration of depositing ions to attain the condition indicated. Large electrodes will thus be less likely to show the phenomena.

Thus, with $V_{sol} \sim 100\ cm^3$, $V_{met} = 8.8\ cm^3\,mol^{-1}$, $C_0 = 10^{-4}$ moles l^{-1}, $\delta = 10^{-3}$, 5×10^{-3} M is sufficient impurity concentration. With $r = 0.3$ mm, the required impurity concentration is six times larger and unreasonably large impurity concentrations for switch on times ~ 100 days are necessary.

COMPARISON WITH EXPECTATIONS FROM PLASMA PHYSICS

When, in the plasma state, two deuterons collide, the products are helium and neutrons or tritium and hydrogen depending upon the mutual orientation of the two ions upon collision. This would be random in the plasma. But at the electrode, the deuteron, during its acceleration across the thin gas layer, will be subject to a vectorial force which will cause it to orient preferentially. One of the two branches will then be favored.

The deuteron is known to be a loosely bound entity, the wave function of which may effectively extend to 20 Fermi. When a deuteron is incident on the surface, it feels a strong negative electric field ($\sim 2 \times 10^9\ V\,cm^{-1}$) because of the pure negative excess surface electric charge. The electric field leads to an effective polarization of the deuteron or a p-wave component term in the deuteron's internal wavefunction. However, when this deuteron is close to the classical turning point, it will experience a strong positive electric field ($> 10^{12}\ V\,cm^{-1}$). This field forces the incident deuteron to reverse its orientation in a specific manner. The deuteron would gain the energy in such a fast reversal of the electric field. Then, the angular momentum of the incident deuteron may be excited from the $J = 0$ state to $J = 2$ or even partly to $J = 4$ states. This fast ($\sim 10^{-17}$ s) reversal of

orientation may loosen the structure of the deuteron nucleus and cause the wave function of the deuteron to be extended to a much larger range. This extension may create a condition which will favor a Philips–Oppenheimer type stripping reaction—the tunneling neutron transfer reaction $D + D \rightarrow T + P$ [30]. The reasons for this kind of stripping reaction are (1) the orientation may help the neutron transfer process; (2) the proton transfer reaction has to penetrate an extra Coulomb barrier compared to the neutron transfer process.

FACTORS LIKELY TO INCREASE FLEISCHMANN–PONS EFFECTS

(1) Pd or alkaline solutions may not be necessary. The metal has to exhibit a Volmer–Heyrovsky path with coupled electrochemical desorption in rate control, because this mechanism of deuterium evolution gives surfaces completely covered with D at high current densities.

(2) Surfaces should be spiky. The tip radii should be minimal [31]. The promontories must grow for a time long enough to penetrate the diffusion layer of the flat electrode.

(3) Surface states should be promoted.

(4) Any method which causes the field in the double layer to fluctuate (e.g. heterodyne beats of superimposed a.c.) would be advantageous.

(5) The working region for D_2 evolution should be as far as possible negative to the electrode p.z.c. of the dendrite forming material.

The most needed information concerns the influence of Li, gas phase tritium production and He. X-ray and γ emission during the rare bursts should be sought.

CONCLUSIONS

(1) The Fleischmann–Pons effects (heat and tritium) have been observed in around one quarter of the electrodes used in the cathodic evolution of deuterium *after very long times*. The success rate improves greatly—up to 70% for T—if the electrode diameter is ~ 1 mm or less.

(2) Tritium reaches 10^4–10^7 disintegration $min^{-1}\,ml^{-1}$ in the solution. Bursts of T last for *ca* 5–50 h.

(3) The tritium increases to steady state concentration in solution over ~ 12 h.

(4) There is a weak suggestion for some correlation between heat and tritium though the two phenomena have only been observed together in one system.

(5) The frequency with which the phenomena are observed falls as the electrode size increases. No effects have been observed when the electrode diameter exceeded 4 mm.

(6) The repeated formation of tritium from deuterium establishes the nuclear nature of the sporadic effects occurring. No non-nuclear explanation for the heat has yet been found [3].

(7) It is difficult to justify a fugacity of D in Pd of $> 10^6$ atm. Fusion *within* Pd is therefore unlikely.

(8) D^+ ions are made from D_2O in the double layer during dielectric breakdown which begins near tips of promontories of foreign material growing on the electrode surface. Reasonable numerical agreement with experiment arises if the effective mass of the deuteron is as small as 0.01 or the electric field at the dendrite tip is $\sim 2 \times 10^9\,V\,cm^{-1}$, or some combination of reduced effective mass and enhanced field.

(9) The model explains the long delay times, the sporadicity and the size effects. It may explain the high branching ratio.

Acknowledgement—We are grateful for financial support from the Electric Power Research Institute (EPRI), the Welch Foundation, and Texas A&M University. It should be pointed out that Mr Zoran Minevski has been taking care of the running of the cells since November 1989, for which we are grateful. We are also grateful for extensive and frequent discussions with Prof. Kevin Wolf of the Cyclotron Institute, Texas A&M University (it was Prof. Wolf who led the search for contamination). We have also gained by technical discussions with Dr David Worledge of EPRI, and Prof. J. Natowitz of the Cyclotron Institute. Thanks are also due to Dr Dennis Corrigan of General Motors, and Drs Robert Sherman, Carol Talcott, Ed Storms and Malcolm Fowler of LANL. We thank our colleagues and co-workers in the Surface Electrochemistry Group for their help in the experimental work, particularly the all-night work in the period April–July 1989.

REFERENCES

1. M. Fleischmann, S. Pons and M. Hawkins, *J. Electroanal. Chem.* **261,** 301 (1989); **263,** 187 (1989).
2. S. E. Jones *et al.*, *Nature* **338,** 737 (1989).
3. R. C. Kainthla, M. Szklarczyk, L. Kaba, G. H. Lin, O. Velev, N. J. C. Packham, J. C. Wass and J. O'M. Bockris, *Int. J. Hydrogen Energy* **14,** 771 (1989).
4. N. J. C. Packham, K. L. Wolf, J. C. Wass, R. C. Kainthla and J. O'M. Bockris, *J. Electroanal. Chem.* **270,** 451 (1989).
5. F. J. Mayer, *Proc. Workshop on Cold Fusion Phenomena*, Santa Fe, NM (May 1989).
6. M. Gajda, D. Harley, J. Rafelski and M. Sawicki, *Proc. Workshop on Cold Fusion Phenomena*, Santa Fe, NM (May 1989).
7. K. Nagamine *et al.*, *Proc. DOE Workshop on Cold Fusion Phenomena*, Sante Fe (1989).
8. M. Rabinowitz and D. H. Worledge, Private communication to G. H. Lin, (September, 1989).
9. C. DeW. Van Siclen and S. E. Jones, *J. Phys. G: Nucl. Phys.* **12,** 213 (1986).
10. A. Farkas, *Trans. Faraday Soc.* **33,** (1937) 552.
11. D. Corrigan, Private communication to J. O'M. Bockris (August 1989).
12. O. Velev and R. C. Kainthla, Submitted to *Fusion Technol.* (1990).
13. J. O'M. Bockris, M. A. Genshaw and M. Fullenwider, *Electrochim. Acta* **15,** 47 (1970).
14. K. L. Wolf, N. J. C. Packham, D. Lawson, J. Shoemaker, F. Cheng and J. C. Wass, *Proc. Workshop on Cold Fusion Phenomena*, Santa Fe, NM (May 1989).
15. P. K. Iyengar, *Fifth Int. Conf.* Emerging Nuclear Energy Systems (ICENES V), Karlsruhe, West Germany (July 1989).
16. T. Mizuno, Private communication to J. O'M. Bockris (October 1989).

17. P. K. Subramanyan in J. O'M. Bockris, B. E. Conway, E. Yeager and R. E. White (eds), *Comprehensive Treatise of Electrochemistry*, Volume 4, p. 411. Plenum Press, New York (1981).
18. J. O'M. Bockris and A. K. N. Reddy, *Modern Electrochemistry*, Volume 1, p. 134. Plenum Press, New York (1973).
19. P. K. Subramanyan and J. O'M. Bockris, *Electrochim. Acta* 16, 2169 (1971).
20. P. McIntyre, Private communication to G. H. Lin (March 1989).
21. F. A. Lewis, *The Palladium Hydrogen System*. Academic Press, New York (1967).
22. K. I. Popov and M. D. Maksimovic, in J. O'M. Bockris *et al.* (eds), *Modern Aspects of Electrochemistry*, Volume 19, p. 193. Plenum Press, N.Y. (1989).
23. W. A. Adams, E. E. Criddle, G. Jerkiewicz, B. E. Conway, V. S. Donepudi and J. Hebert, *Proc. Electrochem. Soc. Meeting*, Hollywood, Florida (October 1989).
24. D. M. Kolb and C. Franke, Submitted to *J. Appl. Phys.* (1989).
25. M. Szklarczyk, R. C. Kainthla and J. O'M. Bockris, *J. Electrochem. Soc.* **136,** 2512 (1989).
26. W. Schmickler and E. Henderson, *J. Phys. Chem.* **85,** 1 (1986).
27. Y. E. Kim, *Proc. First Annual Conf. Cold Fusion*, Salt Lake City, UT (March 1990).
28. S. Srinivasan and A. J. Appleby, Private communication to J. O'M. Bockris (July 1989).
29. J. O'M. Bockris, *Modern Aspects of Electrochemistry*, Volume 1. Butterworths, London (1954).
30. J. R. Oppenheimer and M. Philips, *Phys. Rev.* **48,** 520 (1935).
31. J. L. Barton and J. O'M. Bockris, *Proc. R. Soc.* **A268,** 485 (1962).